

REACTIVITY SCALES AS COMPARATIVE TOOLS FOR CHEMICAL MECHANISMS: SAPRC VS MCM

^aR.G. (Dick) Derwent, ^bM.E. Jenkin, ^cM.J. Pilling

^{*a}rdscientific, Newbury, Berkshire, United Kingdom

^bAtmospheric Chemistry Services, Yelverton, Devon, United Kingdom

^cSchool of Chemistry, University of Leeds, Leeds, United Kingdom

Abstract

An extended version of the Master Chemical Mechanism v3.1 has been used to develop a reactivity scale for the conditions appropriate to California, United States of America using a photochemical trajectory model. The reactivity values, termed Photochemical Ozone Creation Potentials (POCPs), have been compared with the Maximum Incremental Reactivity (MIRs) determined elsewhere with the Statewide Air Pollution Research Center (SAPRC-07) chemical mechanism. The comparison of POCPs and MIRs has been completed for 121 organic compounds representing the alkanes, alkenes, aldehydes, ketones, aromatics, oxygenates and halocarbon classes. Both mechanisms have constructed a consistent and coherent description of reactivity within each class of organics. The extended MCMv3.1 and SAPRC-07 mechanisms appear to have represented the available body of understanding concerning the atmospheric oxidation of organic compounds within each class in a consistent and quantitative manner.

1. Introduction

It is well recognised that each of the hundreds to thousands of organic compounds reacts in the sunlit atmosphere, in the presence of nitrogen oxides (NO_x) to produce different amounts of ozone (Bowman and Seinfeld, 1994). Organic compounds may be classed as reactive if they produce copious amounts of ozone quickly and

unreactive if they react so slowly as to produce minimal amounts. By distinguishing between more reactive and less reactive organic compounds, it may be possible to develop control regulations and strategies that will decrease ozone more efficiently than if all organic compounds are tackled without distinction. A reactivity scale is an ordered list of the ozone productivities of a number of organic compounds determined under comparable conditions that can be used to target control regulations on the more reactive organic compounds. Dimitriades (1996; 1999) describes how reactivity issues have been important in the formulation of policies within the United States of America on the control of organic emissions for ambient ozone reduction.

Different organic compounds show different reactivities because they react differently in the atmosphere. Dimitriades (1996) describes the issues that control the ozone-forming potential of different organic compounds. Each organic compound reacts with hydroxyl (OH) radicals at a different rate. The competition between the different organic compounds for OH is controlled, in part, by the rate coefficients, k_{OH} , for their reactions with OH. The k_{OH} reactivity of an organic compound is an intrinsic property of that compound and can be measured in the laboratory. It can be used to define a reactivity scale, which on a mass emitted basis, would be a set of k_{OH}^i/MW^i values for each compound where MW^i is the molar mass of that compound, i . This is the k_{OH} reactivity scale.

Ozone productivity, however, is not just a question of the speed at which the organic compound reacts, its kinetic reactivity. It is also a question of the mechanism by which it reacts, its mechanistic reactivity (Carter and Atkinson, 1989). Information on kinetic and mechanistic reactivity is usually presented in the form of an atmospheric

chemical mechanism. Reactivity scales are generated from atmospheric chemical mechanisms using simulations of ozone formation under typical ambient conditions and are ordered lists of the ozone productivities of a number of organic compounds, determined under identical conditions (Carter, 1994a). They are therefore compact and concise ways of compiling and summarising large bodies of understanding of the mechanisms of atmospheric chemical reactions.

In this study, a near-explicit chemical mechanism based on the Master Chemical Mechanism (MCM) (Jenkin et al., 1997) has been used to compile a reactivity scale for conditions appropriate to the State of California, United States of America. This reactivity scale, the Photochemical Ozone Creation Potential (POCP) scale, (Derwent et al., 2001) has then been compared with the Maximum Incremental Reactivity (MIR) scale, determined elsewhere (Carter, 2008) with the Statewide Air Pollution Research Center (SAPRC-07) mechanism. The aim of this comparison is to learn about the similarities and differences between the MCM and SAPRC-07 chemical mechanisms. This comparison is inevitably partial, in that it focuses only on ozone productivity. There will be many differences in detail between these two particular atmospheric chemical mechanisms that will have little or no impact on ozone productivity which this study will not, however, illuminate.

In the sections that follow, we begin with a description of the Photochemical Trajectory Model (PTM) and the MCM that drives it. We then describe how the POCP reactivity scale has been generated from it using ambient conditions appropriate to the California situation. The POCP and MIR reactivity assignments for 121 organic compounds are then taken on a class-by-class basis and the similarities

and differences are discussed in terms of the main mechanistic features. It has been important to resolve whether any of the differences found represent real mechanistic differences of policy significance.

2. Determination of a POCP Reactivity Scale for California Conditions

2.1 Photochemical Trajectory Model PTM

The PTM model describes the chemical development within an air parcel that follows an air mass trajectory, forwards in time, reaching an arrival point within a California air basin at the end of a single day's photochemistry (Derwent et al., 1996; Derwent et al., 2001). The rate of change of the concentration of species, c_i , in molecule $\text{cm}^{-3} \text{s}^{-1}$ was described by a series of differential equations of the form in equation (1) below:

$$dc_i/dt = P_i - L_i c_i - V_i c_i/h + E_i/h - (c_i - b_i) \cdot 1/h \cdot dh/dt \quad (1)$$

where P_i is the instantaneous production of species i from photochemistry, $L_i c_i$ is the instantaneous loss rate from photochemistry, V_i is the species dependent dry deposition velocity, h , the time-dependent boundary layer depth, b_i is the aloft concentration of the species and E_i the local areal emission rate of the pollutant sources in molecule $\text{cm}^{-2} \text{s}^{-1}$.

2.2 Master Chemical Mechanism

The production, P_i and loss, $L_i c_i$ terms in equation (1) above, were represented using the Master Chemical Mechanism (MCM), a near-explicit chemical mechanism

describing the detailed degradation of a large number of emitted organic compounds and the resultant generation of ozone and other secondary pollutants under conditions appropriate to the atmospheric boundary layer. The version used in the present study is an extended version of the MCMv3.1 which treats the degradation of methane and 176 organic compounds (Derwent et al., 2007). The base mechanism used, MCMv3.1 can be accessed via the University of Leeds website:

<http://www.chem.leeds.ac.uk/Atmospheric/MCM/mcmproj.html>

and was developed using published mechanism development protocols (Jenkin et al., 2003; Saunders et al., 2003; Bloss et al., 2005). This base mechanism included 136 primary organic compounds and a further 9 organic compounds which are included in the MCMv3.1 as degradation products. Those organic compounds whose atmospheric emissions were negligible under European conditions, based on the detailed speciated inventory of Passant (2002), were removed from the base mechanism. They were replaced with a number of additional organic compounds whose degradation mechanisms were constructed using methods based on those applied within the Common Reactive Intermediates mechanism (Jenkin et al., 2008). The full extended mechanism contains 12,871 reactions and involves 4,414 chemical species.

The photolysis reactions of the photochemically-labile species were calculated from their absorption cross-sections and quantum yield data using a two-stream multiple scattering approach (Hough, 1988). The time-of-the-day dependence of the photolysis rates was described by calculating the instantaneous solar zenith angle, z , and using expressions of the form in equation (2) to estimate the photolysis rate, J , for a particular photochemical process:

$$J = I_0 (\cos Z)^m \exp(-n \sec Z) \quad (2)$$

The coefficients, l, m, n were calculated for each process by fitting J values to appropriate function of Z and can be accessed via the University of Leeds website (<http://www.chem.leeds.ac.uk/Atmospheric/MCM/mcmproj.html>).

2.3 Ambient conditions and model input data

Reactivities depend of the nature and chemical properties of the organic compounds. However, they are not geophysical constants and vary significantly with ambient environmental conditions. These ambient conditions have been carefully specified so that the resulting reactivities are appropriate to the conditions found in air basins in the State of California.

The PTM model was set up using indicative ambient conditions from a database of 39 simplified model scenarios designed to represent ozone formation in 39 areas of the United States of America in the 1980s (Baugues, 1990). Of these environmental scenarios, five have been chosen and implemented in the PTM. These scenarios include: “averaged conditions” AVGEPA, “Los Angeles” LOSCA1, “Sacramento” SACCA1, “San Diego” SDOCA1, “San Francisco” SFOCA1. The database provided information describing:

- the location of the given air basin, its latitude and longitude
- the time of year of the scenario
- the diurnal behaviour of the atmospheric boundary layer depth, the air temperature, the water vapour content
- the time-dependent emissions of the organic compounds, NO_x, carbon monoxide, isoprene and α -pinene

- initial concentrations of total organic compounds, NO_x, methane, carbon monoxide, isoprene and α -pinene
- aloft concentrations of total organic compounds, ozone, methane and carbon monoxide.

Each model simulation was run from 0600z until 1800z. The speciation of the initial concentrations of the organic compounds, their aloft concentrations and the time-dependent emissions were held constant between the 5 scenarios and were taken from Carter (1994b). The time-dependent NO_x emissions were scaled with factors that were time-independent but varied between each scenario. The scale factors were increased in steps to obtain the Maximum Incremental Reactivity (MIR) conditions as described by Carter (1994a).

2.4 Determination of POCPs

To quantify the contributions made to photochemical ozone formation by each organic compound, a series of model sensitivity experiments was performed. In each sensitivity experiment, the instantaneous emission of one organic species at each point along the trajectory path was increased in turn. Total organic compound emissions were increased by 40% relative to the base case. The choice of the increase in the emissions was completely arbitrary and had no policy significance. It was a compromise between the requirement to produce results that were above the noise level in the model with the least reactive species but not too large as to take the model out of its linear response range. The ozone increment for ethylene in the “averaged conditions” scenario was 3.9 ppb above a base case ozone mixing ratio of 195 ppb.

The single day trajectory model was then rerun 176 times, once for each organic species and the ozone mixing ratios at the end of the trajectory were noted for each sensitivity experiment. No other model parameters were changed in the sensitivity experiments from their values in the base case experiment.

The ozone mixing ratios at the end of the trajectory in the sensitivity experiments varied considerably between the different experiments and were generally higher than in the base case model experiment. The incremental increase in organic compound emissions thus led to an incremental increase in the ozone mixing ratios at the endpoint of the trajectory which varied with the organic species. This variability was taken as a measure of the propensity for photochemical ozone formation from each organic species. A Photochemical Ozone Creation Potential POCP index (Derwent et al., 1996) was then calculated for each VOC species, *i*, using the formula:

$$\text{POCP}_i = \frac{O_{3i} - O_{3\text{base case}}}{O_{3\text{ethylene}} - O_{3\text{base case}}} \times 100$$

where $O_{3\text{base case}}$ refers to the ozone mixing ratio at the end of the trajectory in the base case, O_{3i} with an additional emission of the i^{th} species and $O_{3\text{ethylene}}$ refers to that with the same mass of ethylene. The organic species ethylene was used as a bench-mark for the POCP scale because its chemical degradation pathways are well-defined, because of its low molecular mass and because it is one of the most important ozone-forming species (Derwent et al., 1998).

Table 1 contains a summary of the POCP determinations made under North American conditions using the extended MCMv3.1. Each entry shows the mean and standard

deviations of the POCPs for the five environmental scenarios. The standard deviation is given merely as an indication of the uncertainty in the POCP resulting from the choice of background environmental conditions. It is not a measure of overall uncertainty and does not reflect the uncertainties in the PTM, MCM and the input data used to drive them. Annex A contains a summary of the reactivity assignments in the POCP and MIR scales for those organic compounds that are common to the extended MCMv3.1 and SAPRC-07 mechanisms. Basic information has also been tabulated for each of the 121 organic compounds from which the k_{OH} reactivity scale values have been compiled.

3. Comparison of Reactivity Scales

3.1 Comparison of the reactivities for the alkanes

POCPs and MIRs increase with increasing carbon number within the alkane class, from C_2 to a maximum at C_6 on both scales, see Figure 1. Reactivities then decline from C_6 to C_{12} . Reactivity estimates using the k_{OH} scale increase steadily with carbon number from C_2 to C_{12} . Reactivities using the k_{OH} scale follow the POCP and MIR scales initially from C_2 to C_6 but do not show the decline in reactivity above C_6 found in the latter scales. Figure 1 illustrates the difference between kinetic and mechanistic reactivity. The increasing reactivity of the alkanes with carbon number from C_2 to C_6 follows on directly from the increasing reactivity with OH radicals in the parent organic compound. This is straightforwardly described by all three scales. However, for C_6 and higher, the steady increase in OH reactivity shown by the k_{OH} scale has been offset by markedly decreasing mechanistic reactivity as shown by the POCP and

MIR scales. The alkanes above C₆ exhibit a change in their primary degradation pathway which markedly inhibits photochemical ozone formation despite increasing OH reactivity. This change in degradation pathway involves alkoxy radical isomerisation through a six-membered transition state which is favoured for C₆ and higher alkoxy radicals and not favoured for smaller carbon chain lengths. This alkoxy radical isomerisation leads to the formation of hydroxyl-substituted peroxy radicals which exhibit a reduced propensity to drive ozone formation compared with unsubstituted peroxy radicals. This reduced propensity becomes more marked with increasing carbon number reflecting the increasing formation of hydroxyl-substituted alkyl nitrates. All these detailed mechanistic features have been captured quantitatively in both the POCP and MIR scales but not in the k_{OH} scale.

Figure 2 presents a scatter plot of the POCPs and MIRs for the alkane class. Error bars have been provided for the POCPs based on the standard deviations for the five scenarios as given in Table 1. Error bars for the MIRs have been assumed arbitrarily to be ± 30% merely to provide an indication of likely uncertainty range. The aim of the figure is to show how well both reactivity scales agree within this class of organic compounds. Also shown is an orthogonal regression line, representing the fit between the two sets of reactivity assignments. The straight line has the equation:

$$\text{MIR} = 0.0558 \pm 0.006 \text{ POCP} + 0.04 \pm 0.11; R^2 = 0.84.$$

The scatter plot shows that there is a large degree of conformity between the two scales. It is concluded that both the extended MCMv3.1 and the SAPRC-07 mechanisms have processed the available literature kinetic and mechanistic data to

produce the same structural variation in alkane reactivity with carbon number within the likely uncertainty ranges.

3.2 Comparison of the reactivities for the alkenes

Both scales agree that the alkenes as a class are amongst the most reactive of all the classes of organic compounds evaluated. Because they are highly reactive, kinetic reactivity is so high that almost all the alkenes are consumed completely by OH radicals close to their points of emission. Their propensity to form ozone is thus largely controlled by their mechanistic reactivities which differ markedly between the members of the alkene class.

Figure 3 illustrates the influence of kinetic and mechanistic reactivities by plotting out the POCPs and MIRs against their reactivities on the k_{OH} scale. Neither the POCPs nor the MIRs increase monotonically with increasing k_{OH} reactivity. This shows the dominant influence of mechanistic reactivity compared with kinetic reactivity. Interestingly, apart from a scaling factor, the POCPs and MIRs follow each other closely, showing a similar pattern of behaviour with similar deviations from a simple monotonic relationship with k_{OH} reactivity.

Figure 4 presents a scatter plot of the POCPs and MIRs for the alkene class. Again, error bars have been provided for the POCPs based on the five scenarios and taken from Table 1 whilst those of the MIR scale have assumed an arbitrary $\pm 30\%$. Also shown is an orthogonal regression line through the reactivity assignments, with the equation:

$$\text{MIR} = 0.075 \pm 0.017 \text{ POCP} - 0.55 \pm 2.1; R^2 = 0.50$$

There is a high degree of conformity between the POCP and MIR reactivity assignments. It is concluded that both the extended MCMv3.1 and the SAPR-07 chemical mechanisms have been able to characterise similar mechanistic reactivities for the members of the alkene class.

However, not all of the reactivity assignments in Figure 4 lie close to the orthogonal regression. Even with the large error bars assigned to both the two reactivity scales, the points representing α -pinene, β -pinene, limonene, methacrolein and isoprene appear well removed from the line. It would appear that the POCPs for these compounds have been overestimated by between $\pm 50\%$ and a factor of two or that the MIRs have been underestimated by similar factors. Such discrepancies are larger than the likely uncertainties and warrant further investigation.

In previous studies with the MCM, Pinto et al., (2005) discussed the quantum yield data used for methacrolein and recommended that they should be updated.

Accordingly, we have scaled these quantum yields by 0.12 and found that this decreased the POCP for methacrolein by about 7% to the values reported in Tables 1 and A.1. Pinho et al., (2005) reported an important effect on the MCM simulations from updating these quantum yields but this has not been realised in these ambient simulations.

The discrepancies noted for isoprene between the POCP and MIR scales are worthy of comment in view of the favourable comparisons found between the MCMv3.0 and SAPRC-99 mechanisms in the chamber experiments reported by Pinho et al., (2005).

It is possible that there have been more recent changes in the mechanisms that have caused them to diverge.

Degradation mechanisms for complex organic compounds such as α -pinene, β -pinene and limonene are currently incomplete and lack the detailed understanding that is required for their representation in chemical mechanisms. As discussed by Pinho et al., (2007), the degradation chemistry of such large and complex organic compounds includes a large number of sequential and parallel steps of which only those of the first generation reaction products have been characterised in any detail. The divergence of the reactivity estimates between the extended MCMv3.1 and SAPRC-07 reflects differing treatments of this secondary chemistry. In this respect, chamber experiments specifically targeting known degradation products would provide additional information to help develop and evaluate the detailed formulation of their atmospheric degradation.

3.3 Comparison of the reactivities for the aldehydes and ketones

Methyl glyoxal is found to be the most highly reactive organic compound in this class on both scales. Both scales agree also that acetone is the least reactive. The position of acetone as the least reactive ketone on both the MIR and POCP scale is noteworthy in view of the exclusion of acetone as a reactive organic compound by the US EPA (1994).

There is a general increase in POCP and MIR reactivity with increasing k_{OH} reactivity and this is reflected in an exactly analogous manner in the two scales as shown in

Figure 5. The high reactivity of methyl glyoxal found in the POCP and MIR scales is, however, not apparent in the k_{OH} scale. This is because the origin of the high reactivity of methyl glyoxal arises from its photodissociation to radicals rather than its degradation by OH.

Generally speaking, the reactivity assignments made in the POCP and MIR scales follow each other closely as shown in Figure 6. This means that the representations of the mechanistic reactivities of the aldehydes and ketones in the MCM and SAPRC chemical mechanisms agree closely. Also shown in Figure 6 is an orthogonal regression line through the reactivity assignments which has an equation of the form: $MIR = 0.095 \pm 0.019 POCP + 0.38 \pm 1.34; R^2 = 0.70$

It is concluded that both the extended MCMv3.1 and the SAPRC-07 chemical mechanisms have been able to characterise the reactivities of the majority of the aldehydes and ketones in a consistent quantitative manner.

There is, however, one reactivity assignment, that for glyoxal, which is well removed from the generally close fit as demonstrated with the orthogonal regression line. Either the POCP appears to be underestimated by about a factor of 2.5 or the MIR is similarly overestimated. One of the major oxidation products of glyoxal in the extended MCMv3.1 mechanism is glypan, $HCOCOO_2NO_2$, formed by the reaction of NO_2 with $HCOCOO_2$. Experimental studies cast doubt on the existence of glypan (Orlando and Tyndall, 2001) and this aspect of the atmospheric chemistry of glyoxal will be updated during the preparation of the next version of the MCM. Updating the glyoxal oxidation mechanism caused a 25% increase in the POCP to the values reported in Tables 1 and A.1. This has not been enough to resolve the discrepancies

between the POCP and MIR values. Further work is therefore required to improve the representation of the atmospheric chemistry of glyoxal in chemical mechanisms.

3.4 Comparison of the reactivities for the aromatics

It is well recognised that the chemical mechanisms describing the OH reaction and subsequent degradation of the aromatic compounds and hence their role in ozone formation, are not well understood. This is contrast to the situation for the alkanes, alkenes, aldehydes and ketones that have been the subject of sections 3.1 to 3.3 above. As a consequence of this lack of understanding, it is anticipated that this will be reflected in different representations of aromatic chemistry within the extended MCMv3.1 and SAPRC-07 chemical mechanisms. These different representations may well lead to differences in reactivities generated by the two mechanisms.

Table 1 summarises the POCPs determined here for the aromatics as a class. POCPs range from -119 ± 166 for phenol up to 188 ± 49 for 1,2,3,5-tetramethylbenzene. This is the widest range found for any class of organic compounds studied. Considering the sub-set of alkylbenzenes, then POCPs range for 1 ± 6 for the unreactive benzene to 188 ± 49 for the tetra-substituted alkylbenzene and, again, this is a considerable range in reactivity. The POCPs differ markedly depending on the pattern of alkyl substitution on the aromatic ring. Multi-alkyl substitutions appear to increase reactivity versus mono-alkyl substitution for the same carbon number. So, for example, ethylbenzene is much less reactive compared with the xylenes.

The POCPs and MIRs for the alkylbenzenes follow the same overall pattern, with benzene the least reactive and the tri- and tetra-methyl benzenes being the most highly reactive. POCPs and MIRs thus increase with increasing k_{OH} reactivity as is demonstrated in Figure 7. However, for three aromatics: benzaldehyde, o-cresol and styrene, marked deviations from their k_{OH} reactivities are found in both their POCP and MIR reactivities. For these species, mechanistic reactivity controls overall reactivity and not kinetic reactivity.

A scatter plot of the MIRs and POCPs for the aromatics is shown in Figure 8. There is a close association between the two sets of reactivities. This could only have arisen if the two mechanisms share a common understanding of the mechanistic factors that control the differences in reactivity between the different members of the aromatics class. Also shown in Figure 7 is an orthogonal regression line fitted through the reactivity assessments. The equation of the fitted line is:

$$\text{MIR} = 0.042 \pm 0.0047 \text{ POCP} + 2.62 \pm 0.45; \quad R^2 = 0.75.$$

The orthogonal regression is thus able to account for a significant fraction of the variance in the reactivity assessments. This fraction is significantly higher than that accounted for by the corresponding regressions for the alkenes, aldehydes and ketones.

However, not all of the reactivity assessments lie close to the orthogonal regression as is shown by the point for phenol. The mean and standard deviation for the POCP for phenol is -119 ± 166 over the five scenarios. The width of the error bars for phenol in Figure 7 demonstrates that the POCP has not been well-defined over the five scenarios. This is because phenol oxidation and degradation acts as a potent NO_x sink

and this reduces the availability of NO_x to drive ozone production from all other organic compounds. Hence phenol has a negative POCP. A further consequence is that the POCP is markedly sensitive to the background NO_x environment as defined by the five scenarios. It is likely then that the reactivity of phenol is highly mechanism and background environment dependent. It is subject to considerable uncertainty and the reactivity of phenol is thus not adequately characterised in the POCP scale.

It is concluded that, despite the limited understanding of the detailed aromatics mechanisms, both the extended MCMv3.1 and the SAPRC-07 mechanisms have been able to reach a common understanding of the differences in mechanistic reactivity within the members of the aromatics class. This common representation has been achieved by entirely independent routes, involving different mechanism generation protocols, procedures and techniques, with a different balance in the selection of laboratory and experimental data. The agreement is heartening and lends some confidence to the application of either reactivity scale in policy applications involving the aromatics. However, it does not guarantee that either mechanism has captured fully the real-world behaviour of the aromatics.

3.5 Comparison of the reactivities for the oxygenates

The oxygenates are an important class of organic compounds in their own right because they contain a high proportion of unreactive and low reactive species. They are therefore a potentially useful class of compounds that can be employed as replacements for more reactive compounds. It is therefore important that there is a measure of coherence between the reactivity scales for this class of compound.

The POCPs for the oxygenates cover the range from close to zero for methyl formate to over 50 for diethylether. The MIRs show a similar ordering of reactivities with esters significantly less reactive compared with ethers. Figure 9 shows how both POCPs and MIRs increase with increasing k_{OH} reactivity. Significant divergences were noted between the POCP and MIR assignments in Figure 9 for three oxygenates: diacetone alcohol, dimethylether and i-propanol. Nevertheless, the broad pattern of reactivity within the oxygenate class was similar in the POCP and MIR scales.

A high degree of coherence between the POCP and MIR reactivity assignments within the oxygenate class is demonstrated in the scatter plot in Figure 10. Also shown is an orthogonal regression fit with an equation:

$$\text{MIR} = 0.0754 \pm 0.006 - 0.043 \pm 0.16; R^2 = 0.87.$$

Of all the classes of organic compounds studied here, the oxygenate class gave the highest R^2 value in the orthogonal regression. This reinforces the point that the POCP and MIR scales offer a coherent assessment of reactivity within the oxygenate class. This must mean that there is a similar level of coherence in the representation of oxygenate chemistry in the extended MCMv3.1 and SAPRC-07 chemical mechanisms.

Despite the overall goodness of fit indicated by the orthogonal regression in Figure 10, notable deviations were observed for diacetone alcohol, s-butanol, propanoic acid and ethylene glycol. These discrepancies warrant further investigation.

3.6 Comparison of the reactivities for miscellaneous organic compounds

The final class of organic compounds contains a miscellaneous selection of organic compounds comprising alkynes, cycloalkanes and halocarbons. The aim is to illustrate the ability of the two mechanisms, MCMv3.1 and SAPR-07, to handle a wide diversity of organic compounds and to demonstrate whether there is any coherence between the reactivity estimates generated using them.

Figure 11 presents a scatter plot of the POCP and MIR reactivity assignments for the organic compounds in the miscellaneous class. Reactivities are highest in both scales for propyne and lowest for tetrachloroethylene, of the compounds studied. An orthogonal regression has been fitted through the reactivity assignments and the fitted line is shown in Figure 11. It exhibits an equation of the form:

$$\text{MIR} = 0.043 \pm 0.011 \text{ POCP} + 0.11 \pm 0.49; R^2 = 0.67.$$

Most of the reactivity assignments scatter close to the orthogonal regression, showing that both chemical mechanisms have a common representation of reactivity for this diverse range of compounds.

However, one reactivity assignment, that for ethylidene dichloride, appears to diverge markedly from the orthogonal regression fit. Either the POCP has been overestimated by about a factor of three or the MIR has been underestimated by a similar factor.

In summary, the reactivity assignments for the miscellaneous class appear largely to be consistent between the POCP and MIR scales.

4. Discussion of the Results

Over the last four decades, a considerable body of understanding has been built up concerning the mechanism of the atmospheric oxidation of organic compounds and hence their contribution to photochemical ozone formation. A driving force behind the development of this understanding has been the characterisation of reactivity scales and their potential use in the formulation of cost-effective strategies for the reduction of ozone exposure levels (Finlayson and Pitts, 1993).

In this study, the focus has been on how two chemical mechanisms: the extended MCMv3.1 and SAPRC-07, have represented this current understanding and the extent to which they have constructed convergent or divergent pictures of the atmospheric oxidation of organic compounds. Both mechanisms are based upon near-explicit representations of the chemical reactions involved and rely heavily on structure-activity relationships to estimate the majority of the rate coefficients required. Their point of departure is in the manner of representation of reaction products. In the MCM, all reactions are represented as fully explicit stoichiometric equations, with stoichiometric product yields. The MCM is termed near-explicit because there is a limit to the representation of the fate and behaviour of minor products without which the mechanism would grow out-of-control (Jenkin et al., 1997; Saunders et al., 2003). In the SAPRC mechanisms, the surrogate species approach is adopted where reaction products are represented by a limited number of hypothetical species with non-stoichiometric yields (Carter, 2008). Both mechanisms employ mechanism generation protocols to define the representation of these reaction pathways and products.

The comparison of two mechanisms such as the extended MCMv3.1 and SAPRC-07 is therefore not straightforward and is not simply a question of working through each mechanism, process-by-process, equation-by-equation or line-by-line for each emitted organic compound. Here, we employ reactivity scales as comparative tools for comparing mechanisms. The central assumption is that a reactivity scale is a numerical representation of the manner in which a chemical mechanism has represented differences in mechanistic reactivity within each class of organic compounds and between the major classes. Kinetic reactivity should have been handled more or less identically between the MCMv3.1 and SAPRC-07 mechanisms because there is little controversy over OH reaction rate coefficient data either from observation or from structure-activity relationships. The use of reactivity scales as comparative tools necessarily focuses attention on ozone and would not necessarily indicate how the mechanisms compared when judged on peroxyacetyl nitrate (PAN), formaldehyde or any other trace organic reaction products.

A reactivity scale, the Photochemical Ozone Creation Potential (POCP) scale, has been constructed here using the extended MCMv3.1 mechanism as described in section 2 above under conditions appropriate to the state of California. The SAPRC-07 mechanism has been used to generate the Maximum Incremental Reactivity (MIR) scale in work described elsewhere (Carter, 2008). In section 3, the POCPs and MIRs have been compared for 121 organic compounds representing the major classes of organic compounds, namely the alkanes, alkenes, aldehydes, ketones, aromatics, oxygenates and halocarbons. Within-class variations in reactivity appear to be consistent between the POCP and MIR scales. Not only do scatter plots indicate excellent correlations between POCPs and MIRs, but POCPs and MIRs diverge in

coherent ways from the corresponding k_{OH} reactivity values. These correlations between the POCPs and MIRs and their coherent divergences from the k_{OH} reactivities could not have been achieved by chance for such a large number of organic compounds. They have arisen because both mechanisms have represented the available body of understanding concerning the atmospheric oxidation of organic compounds within each class in a consistent and quantitative manner.

These observations concerning the correlations between the POCPs and MIRs appear to be equally true for the aromatics as for the other classes of organics. This is heartening because the oxidation mechanisms for the aromatics are considered to be incomplete and unsatisfactory. It appears that both mechanisms have constructed a coherent picture of mechanistic reactivity for aromatics with different patterns of substitution on their aromatic rings and with different alkyl side chains. This level of agreement between the MCMv3.1 and SAPRC-07 mechanisms is important for policy because aromatics are highly reactive and drive a significant fraction of photochemical ozone formation under California conditions.

Not all of the reactivity assignments are consistent between the POCP and MIR scales for all 121 organic compounds studied. A total of 15 organics had POCPs that were apparently inconsistent with their MIRs or vice versa. These organics included 5 alkenes: isoprene, methacrolein, α -pinene, β -pinene and limonene; an aldehyde: glyoxal; 4 aromatics: benzaldehyde, styrene, phenol and o-cresol; 4 oxygenates: diacetone alcohol, s-butanol, propanoic acid and ethylene glycol; and a halocarbon: ethylidene dichloride.

For the 4 aromatics listed above, atmospheric oxidation appeared to be a potent NO_x sink. As a consequence, additional NO_x was removed from the system when additional organic was added to determine its incremental reactivity. This reduced ozone production from all other organic compounds, leading to -ve or close to -ve POCPs. A further consequence was that the POCP was markedly sensitive to the background NO_x environment as shown by the large standard deviations assigned to the POCPs. It is likely then that the POCPs (and presumably the MIRs) are not well-founded for these species and are highly model dependent. For the remaining 11 organic compounds where significant discrepancies were found between the corresponding POCPs and MIRs, it is not thought likely that this indicates a fundamental point of departure between the underlying extended MCMv3.1 and the SAPRC-07 mechanisms. The discrepancies are more likely to have been caused by some species-dependent facets of their atmospheric degradation mechanisms that are not adequately resolved in the available experimental data.

The extended MCMv3.1 and SAPRC-07 mechanisms appear to have represented the available body of understanding concerning the atmospheric oxidation of organic compounds within each class in a consistent and quantitative manner. Where significant differences have been found in the reactivity estimates between the two mechanisms, it is not considered likely that such reactivity differences will have any great impact on policy.

[Acknowledgements](#)

The development of the Photochemical Trajectory Model and the Master Chemical Mechanism was supported by the Air Quality and Industrial Pollution Division of the

United Kingdom Department for Environment, Food and Rural Affairs through contracts EPG 1/3/200, AQ 03508, AQ 0704. M.E.J. acknowledges support from the Natural Environment Research Council (NERC) through the provision of Senior Research Fellowship Grants NER/K/S/2000/00870 and NE/D008794/1.

References

- Baugues, K., 1990. Preliminary planning information for updating the ozone regulatory impact analysis version of EKMA. Source Receptor Analysis Branch, Technical Support Division, U.S. Environmental Protection Agency, Research Triangle Park, North Carolina, USA.
- Bloss, C., Wagner, V., Jenkin, M. E., Volkamer, R., Bloss, W. J., Lee, J. D., Heard, D. E., Wirtz, K., Martin-Reviejo, M., Rea, G., Wenger, J. C. and Pilling, M. J., 2005. Development of a detailed chemical mechanism (MCMv3.1) for the atmospheric oxidation of aromatic hydrocarbons, *Atmos. Chem. Phys.*, 5, 641-644.
- Bowman, F.M, Seinfeld, J.H., 1994. Ozone productivity of atmospheric organics. *Journal of Geophysical Research* 99, 5309-5324.
- Calvert, J.G., Atkinson, R., Kerr, J.A., Madronich, S., Moortgat, G.L., Wallington, T.J., Yarwood, G., 2000. The mechanisms of atmospheric oxidation of the alkenes. Oxford University Press, New York, USA.
- Calvert, J.G., Atkinson, R., Becker, K.H., Kamens, R.M., Seinfeld, J.H., Wallington, T.J., Yarwood, G., 2002. The mechanisms of atmospheric oxidation of aromatic hydrocarbons. Oxford University Press, New York, USA.
- Calvert, J.G., Derwent, R.G., Orland, J.J., Tyndall, G.S., Wallington, T.J., 2008. Mechanisms of atmospheric oxidation of the alkanes. Oxford University Press, New York, USA.

Carter, W.P.L., 1994a. Development of ozone reactivity scales for volatile organic compounds. *Journal of Air and Waste Management Association* 44, 881-899.

Carter, W.P.L., 1994b. Calculation of reactivity scales using an updated Carbon Bond IV Mechanism. Report prepared for Systems Applications International for the Auto/Oil Air Quality Improvement Program.

Carter, W.P.L., 2008. Development of the SAPRC-07 chemical mechanism and updated ozone reactivity scale. Center for Environmental Research and Technology, University of California Riverside, California, USA.

Carter, W.P.L., Atkinson, R., 1989. Computer modelling study of incremental hydrocarbon reactivity. *Environmental Science and Technology* 23, 864-880.

Derwent, R.G., Jenkin, M.E., Saunders, S.M., 1996. Photochemical ozone creation potentials for a large number of reactive hydrocarbons under European conditions. *Atmospheric Environment* 30, 181-199.

Derwent, R.G., Jenkin, M.E., Saunders, S.M., Pilling, M.J., 1998. Photochemical ozone creation potentials for organic compounds in northwest Europe calculated with a Master Chemical Mechanism. *Atmospheric Environment* 32, 2429-2441.

Derwent, R.G., Jenkin, M.E., Saunders, S.M., Pilling, M.J., 2001. Characterization of the reactivities of volatile organic compounds using a Master Chemical Mechanism. *Journal of Air and Waste Management Association* 51, 699-707.

Dimitriadis, B., 1996. Scientific basis for the VOC reactivity issues raised by Section 183(e) of the Clean Air Act Amendments of 1990. *Journal of Air and Waste Management Association* 46, 963-970.

Dimitriadis, B., 1999. Scientific basis of an improved EPA policy on control of organic emissions for ambient ozone reduction. *Journal of Air and Waste Management Association* 49, 831-838.

Finlayson-Pitts, B.J., Pitts, J.N., 1993. Atmospheric chemistry of tropospheric ozone formation: Scientific and regulatory implications. *Journal of Air and Waste Management Association* 43, 1091-1100.

Hough, A.M., 1988. The calculation of photolysis rates for use in global tropospheric modelling studies. AERE Report R 13259, HM Stationery Office, London, UK.

Jenkin M. E., Saunders, S. M., Wagner, V., Pilling, M. J., 2003. Protocol for the development of the Master Chemical Mechanism, MCM v3, Part B: tropospheric degradation of aromatic volatile organic compounds. *Atmospheric Chemistry and Physics*, 3, 181-193.

Jenkin, M.E., Watson, L.A., Utembe, S.R., Shallcross, D.E., 2008. A Common Reactive Intermediates (CRI) mechanism for VOC degradation. Part 1: Gas phase mechanism development. *Atmospheric Environment* 42, 7185-7195.

Orlando, J.J., Tyndall, G.S., 2001. The atmospheric chemistry of the HC(O)CO radical. *International Journal of Chemical Kinetics* 33, 149-156.

Pinho, P.G., Pio, C.A., Jenkin, M.E., 2005. Evaluation of isoprene degradation in the detailed chemical mechanism, MCM v3, using environmental chamber data. *Atmospheric Environment* 39, 1303-1322.

Pinho, P.G., Pio, C.A., Carter, W.P.L., Jenkin, M.E., 2007. Evaluation of α - and β -pinene degradation in the detailed tropospheric chemistry mechanism, MCM v3.1, using environmental chamber data. *Journal of Atmospheric Chemistry* 57, 171-202.

Saunders, S.M., Jenkin, M.E., Derwent, R.G., Pilling, M.J., 2003. Protocol for the development of the Master Chemical Mechanism, MCM v3 (Part A): Tropospheric degradation of non-aromatic volatile organic compounds. *Atmospheric Chemistry and Physics* 3, 161-180.

US EPA, 1994. Air quality: Revision to definition of volatile organic compounds –
Exclusion of acetone. Federal Register 59, No. 189, Friday September 30th.

Table 1. Summary of the POCPs determined here using an extended Master Chemical Mechanism v3.1 under North American conditions.

Species	POCP	Species	POCP
Alkanes		Alkenes	
ethane	3±1	ethylene	100 ^b
propane	9±2	propylene	134±14
butane	18±4	but-1-ene	108±17
i-butane	20±4	cis but-2-ene	165±33
pentane	22±5	trans but-2-ene	173±35
i-pentane	21±4	butylene	97±12
neopentane	10±2	buta-1,3-diene	120±12
hexane	20±4	pent-1-ene	89±15
2-methylpentane	26±5	cis pent-2-ene	145±32
3-methylpentane	25±5	trans pent-2-ene	145±31
2,2-dimethylbutane	13±2	2-methylbut-1-ene	92±10
2,3-dimethylbutane	20±3	3-methylbut-1-ene	89±17
heptane	15±4	2-methylbut-2-ene	155±35
2-methylhexane	19±4	isoprene	173±19
3-methylhexane	24±5	hex-1-ene	92±13
octane	13±5	cis hex-2-ene	127±30
nonane	11±6	trans hex-2-ene	127±30
decane	12±7	α-pinene	109±20
undecane	12±7	β-pinene	70±16
dodecane	12±8	limonene	134±31
		acrolein	80±44
Aromatics		methacrolein	136±41
benzene	1±6	Oxygenates	
toluene	33±8		
o-xylene	79±19	methanol	8±1
m-xylene	94±23	ethanol	17±5
p-xylene	74±17	i-propanol	13±2
ethylbenzene	36±9	propanol	30±6
propylbenzene	26±6	butanol	35±8
i-propylbenzene	29±6	i-butanol	34±2
1,2,3-trimethylbenzene	125±32	sec-butanol	26±5
1,2,4-trimethylbenzene	137±27	3-methylbutan-1-ol	47±3
1,3,5-trimethylbenzene	141±23	diacetone alcohol	21±3
o-ethyltoluene	65±18	methyl formate	1±0
m-ethyltoluene	82±19	methyl acetate	3±1
p-ethyltoluene	60±16	i-propyl acetate	16±3
3,5-dimethylethylbenzene	134±24	n-propyl acetate	15±3
1,2,3,5-tetramethylbenzene ^c	188±49	butyl acetate	14±2

1,2,4,5-tetramethylbenzene ^c	181±47	dimethylether	18±5
1-methyl-3-i-propylbenzene ^c	151±44	diethylether	53±9
3,5-diethyltoluene	121±25	di-i-propylether	41±8
benzaldehyde	-36±34	formic acid	1±0
2-methylbenzaldehyde ^d	-101±83	acetic acid	6±1
3-methylbenzaldehyde ^d	-83±69	propanoic acid	6±2
4-methylbenzaldehyde ^d	-36±43	ethylene glycol	25±5
styrene	7±31	propylene glycol	29±7
phenol	-119±166	2-butoxyethanol	38±7
o-cresol	-20±116	1-methoxy-2-propanol	32±6
2,5-xylene ^d	42±115	2-methoxyethanol	34±3
2,4-xylene ^d	52±95	2-ethoxyethanol	42±5
2,3-xylene ^d	16±105		
		Miscellaneous	
Aldehydes and ketones			
		acetylene	4±0
formaldehyde	78±20	propyne ^c	101±40
acetaldehyde	59±20	cyclohexane	20±5
propionaldehyde	63±24	cyclohexanone	21±5
butyraldehyde	60±21	cyclohexanol	45±10
i-butyraldehyde	60±18	methylene dichloride	1±1
pentanal	74±20	tetrachloroethylene	1±0
3-methylbutanal	73±23	trichloroethylene	14±3
glyoxal	60±16	ethyl chloride	12±5
methylglyoxal	163±44	ethylidene dichloride	91±22
acetone	4±1		
methylethylketone	18±4		
diethylketone	17±5		
methyl-i-butylketone	53±6		

Notes:

- the mean and standard deviations are estimated from the five different scenarios describing the background environmental condition in the state of California from Baugues (1990; 1991).
- ethylene is the index point of the POCP scale which is by definition 100 with a standard deviation of zero. This does not imply that the reactivity of ethylene is completely certain, merely that all other POCPs have been expressed relative to ethylene = 100.
- species treated using the CRI-based approach and so is not described in the same level of detail as the species in the remainder of the table.
- species treated as a degradation product in the base MCMv3.1 mechanism and so is not described in the same level of detail as the species in the remainder of the table.

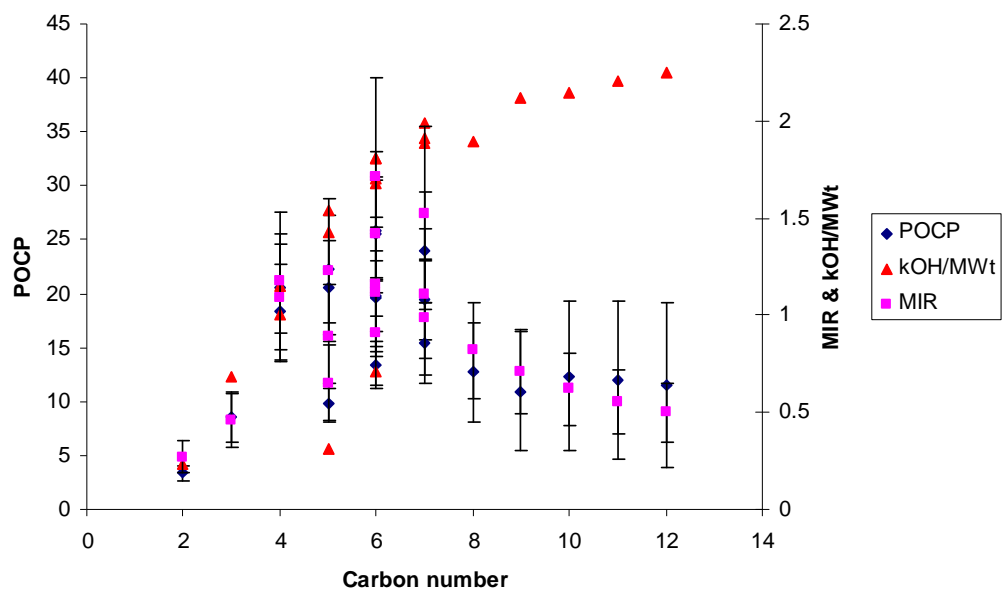


Figure 1. Variation of the reactivity assignments in the k_{OH} , POCP and MIR scales with carbon number for the alkane class. The assignments on the k_{OH} scale have been multiplied by 500 to allow overplotting with the MIRs.

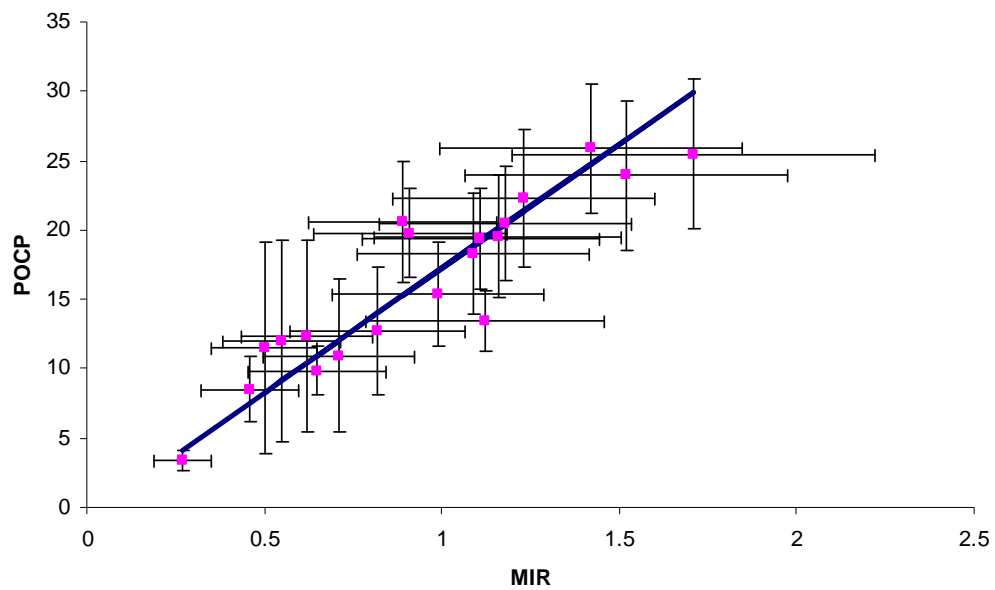


Figure 2. Scatter plot of the reactivity assignments using the MIR and POCP scales for the alkanes, together with an orthogonal regression line through the assignments.

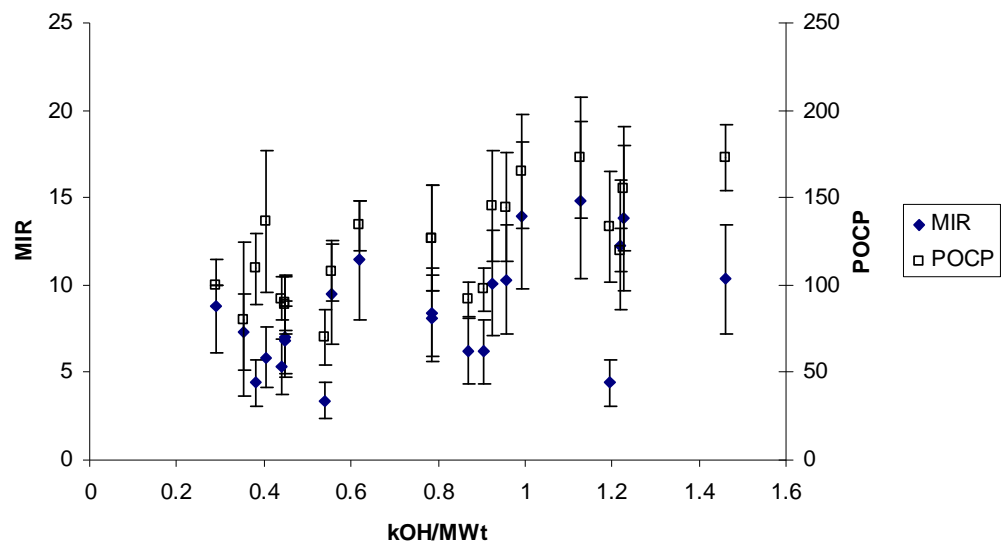


Figure 3. Variation of the reactivity assignments using POCP and MIR scales with those from the k_{OH} scale for the alkene class.

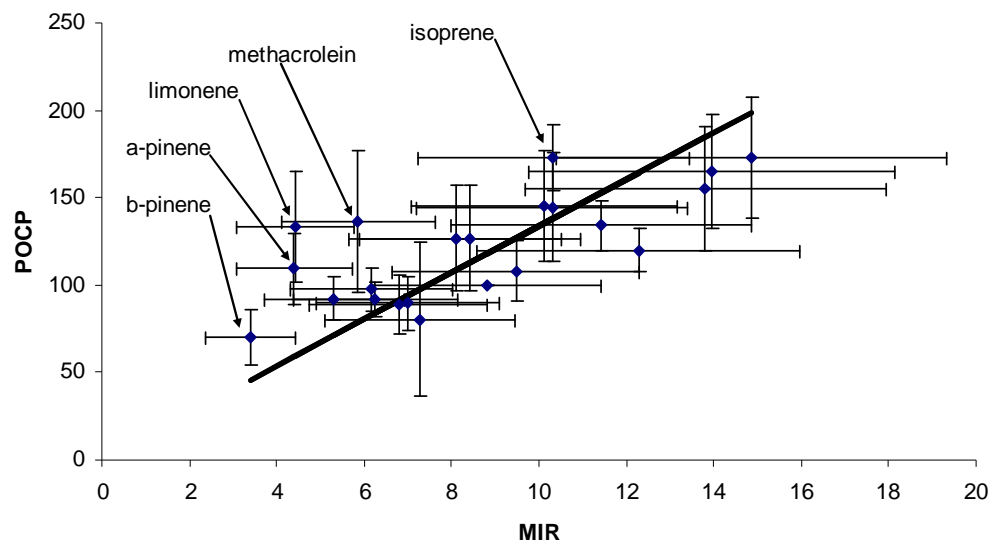


Figure 4. Scatter plot of the reactivity assignments for the alkenes using the MIR and POCP scales, together with an orthogonal regression line through the assignments.

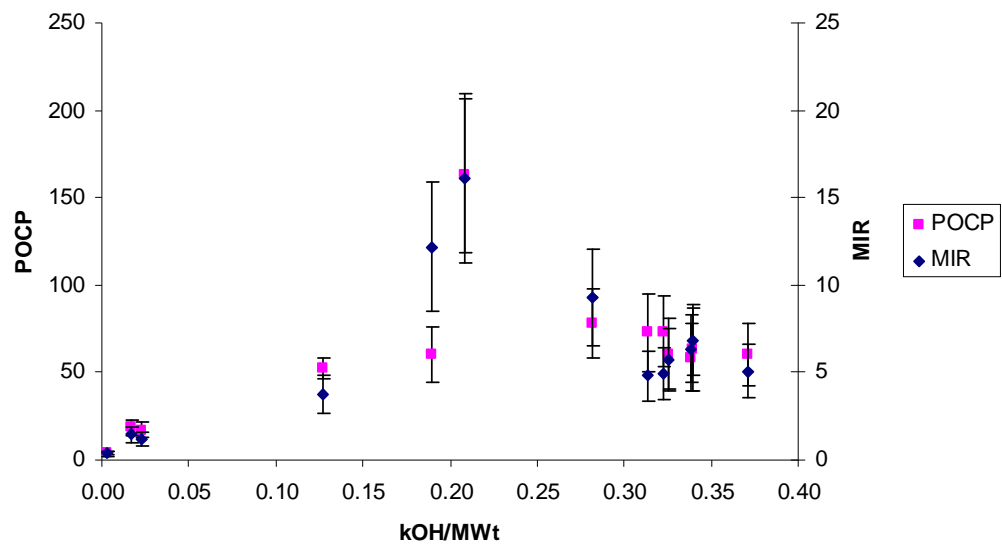


Figure 5. Variation of the reactivity assignments using POCP and MIR scales with those from the k_{OH} scale for the aldehydes and ketones.

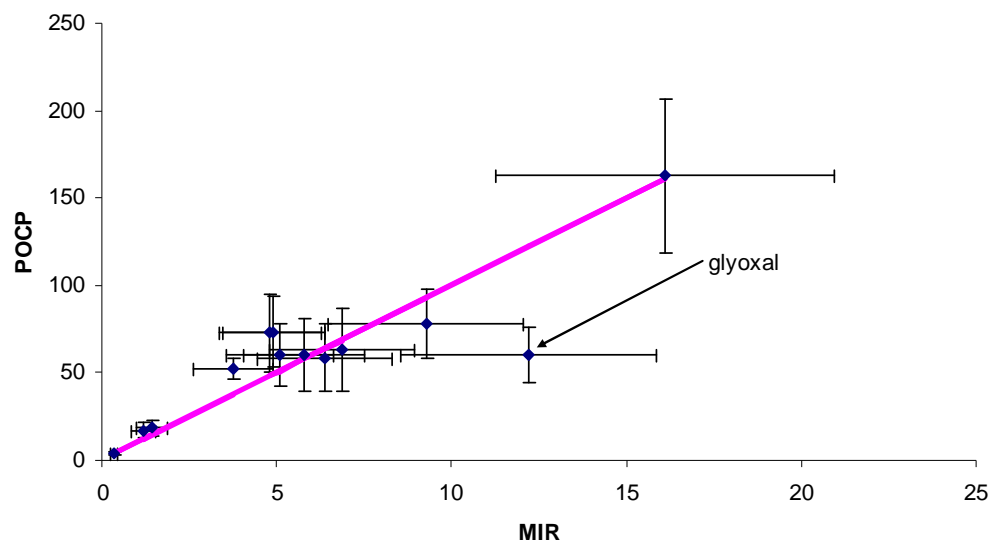


Figure 6. Scatter plot of the reactivity assignments for the aldehydes and ketones in the POCP and MIR scales, showing an orthogonal regression line.

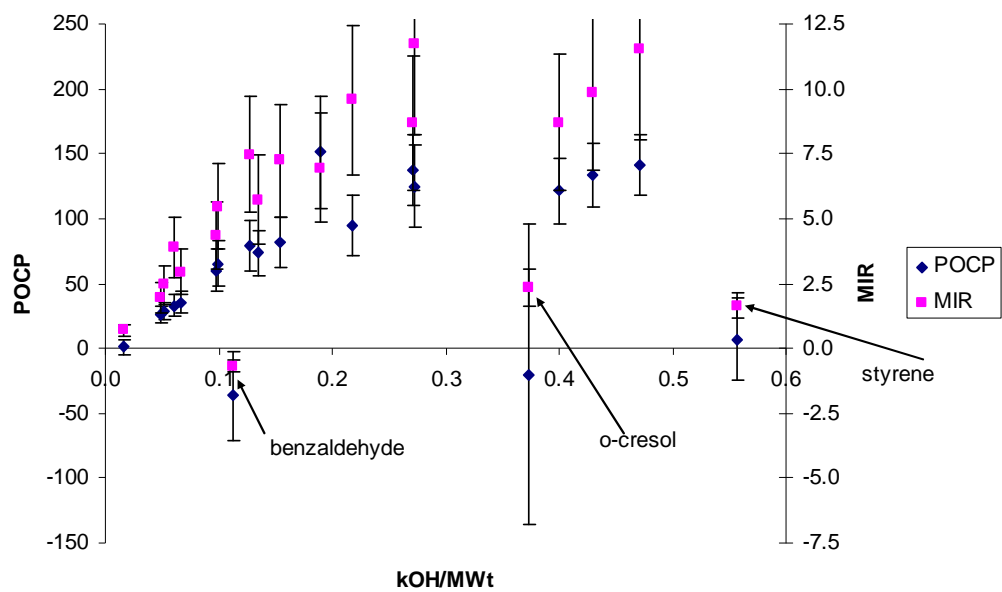


Figure 7. Variation of the reactivity assignments using POCP and MIR scales with those from the k_{OH} scale for the aromatics.

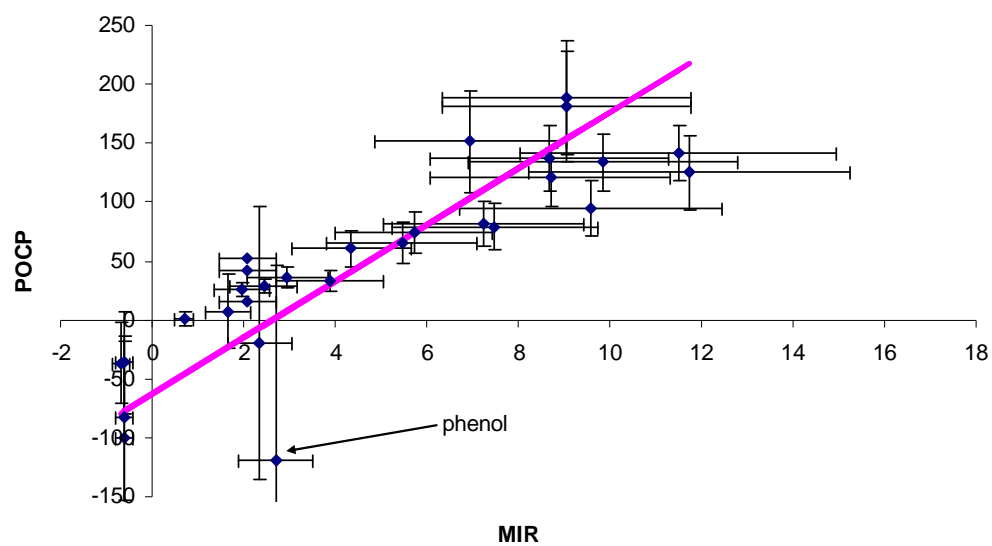


Figure 8. Scatter plot of the reactivity assignments for the aromatics in the POCP and MIR scales, showing an orthogonal regression line fitted through the points.

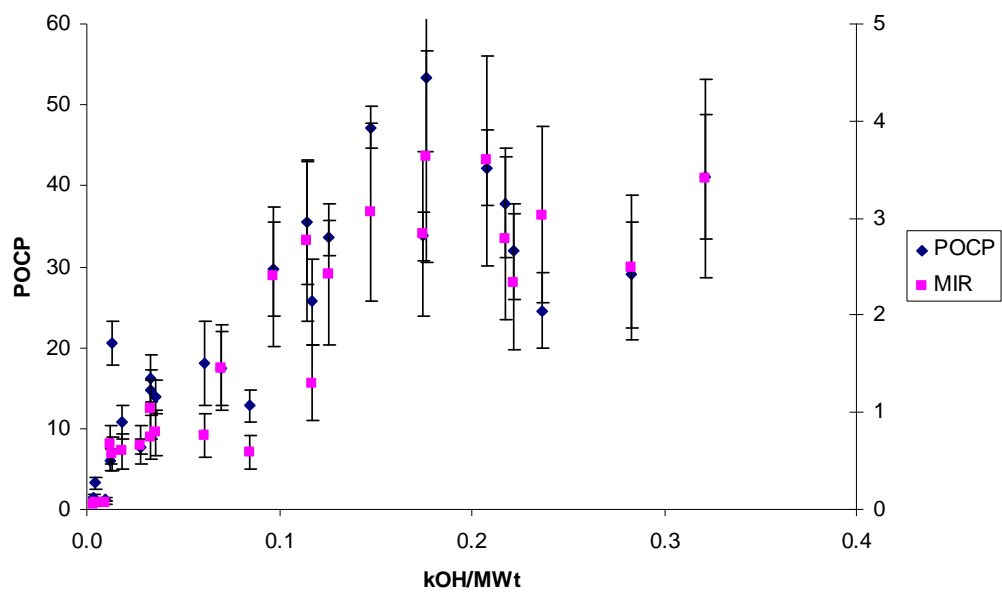


Figure 9. Variation of the reactivity assignments using POCP and MIR scales with those from the k_{OH} scale for the oxygenates.

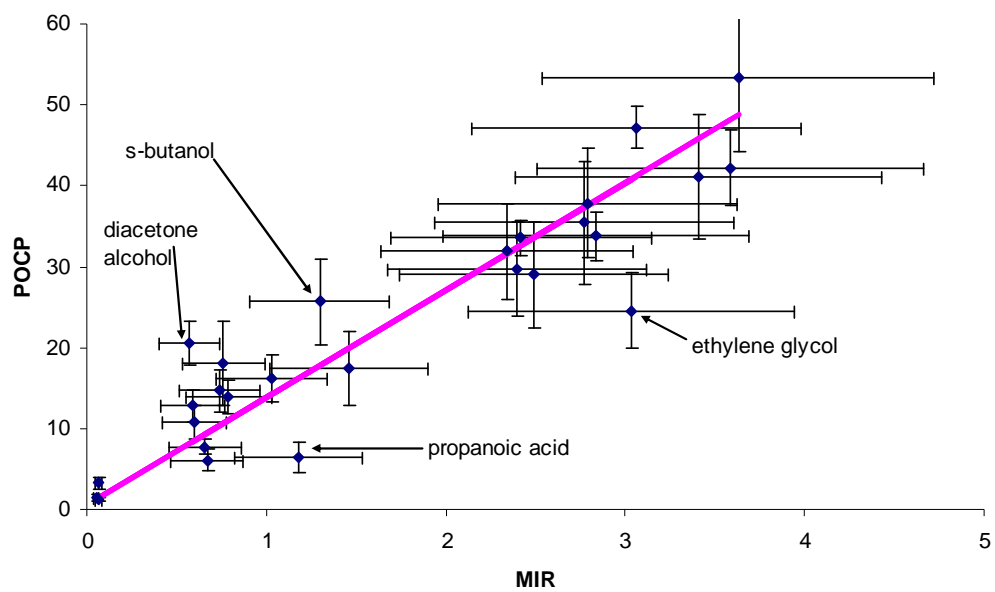


Figure 10. Scatter plot of the reactivity assignments for the oxygenates in the POCP and MIR scales, showing an orthogonal regression line fitted through the points.

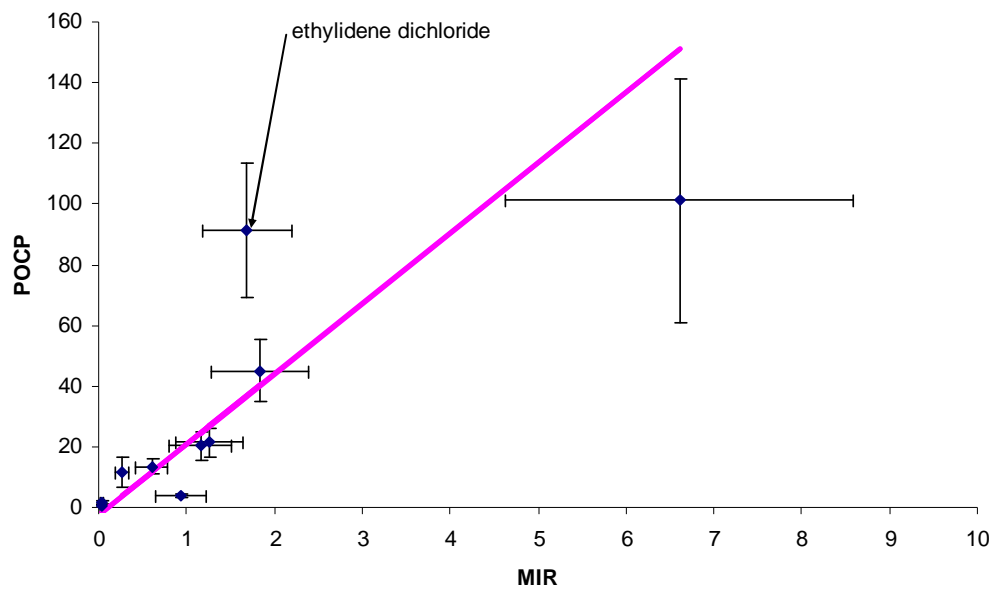


Figure 11. Scatter plot of the reactivity assignments for the miscellaneous class of organic compounds in the POCP and MIR scales, showing an orthogonal regression line fitted through the points.

Annex A. Data compilations and reactivity assignments for a wide range of organic compounds

Table A.1 Data compilations and reactivity assignments using the k_{OH} , POCP and MIR reactivity scales.

		POCP	standard deviation	MIR	carbon number	k_{OH}^c	MWt	k_{OH}/MWt
ethane	alkane	3	1	0.27	2	0.25	30.07	0.0083
propane	alkane	9	2	0.46	3	1.08	44.11	0.0245
butane	alkane	18	4	1.09	4	2.4	58.12	0.0413
i-butane	alkane	20	4	1.18	4	2.1	58.12	0.0361
pentane	alkane	22	5	1.23	5	4	72.15	0.0554
i-pentane	alkane	21	4	0.89	5	3.7	72.15	0.0513
neopentane	alkane	10	2	0.65	5	0.82	72.15	0.0114
hexane	alkane	20	4	1.16	6	5.2	86.18	0.0603
2-methylpentane	alkane	26	5	1.42	6	5.3	86.18	0.0615
3-methylpentane	alkane	25	5	1.71	6	5.6	86.18	0.0650
2,2-dimethylbutane	alkane	13	2	1.12	6	2.2	86.18	0.0255
2,3-dimethylbutane	alkane	20	3	0.91	6	5.6	86.18	0.0650
heptane	alkane	15	4	0.99	7	6.8	100.21	0.0679
2-methylhexane	alkane	19	4	1.11	7	6.89	100.21	0.0688
3-methylhexane	alkane	24	5	1.52	7	7.17	100.21	0.0715
octane	alkane	13	5	0.82	8	7.8	114.23	0.0683
nonane	alkane	11	6	0.71	9	9.8	128.25	0.0764
decane	alkane	12	7	0.62	10	11	142.28	0.0773
undecane	alkane	12	7	0.55	11	12.4	156.31	0.0793
dodecane	alkane	12	8	0.5	12	13.8	170.33	0.0810
ethylene	alkene	100	0 ^a	8.80	2	8.15	28.05	0.290
propylene	alkene	134	14	11.43	3	26.00	42.08	0.618

but-1-ene	alkene	108	17	9.47	4	31.10	56.11	0.554
cis-but-2-ene	alkene	165	33	13.97	4	55.80	56.11	0.995
trans-but-2-ene	alkene	173	35	14.87	4	63.20	56.11	1.126
cis-pent-2-ene	alkene	145	32	10.12	5	65.00	70.13	0.927
trans-pent-2-ene	alkene	145	31	10.30	5	67.00	70.13	0.955
1-pentene	alkene	89	15	7.00	5	31.40	70.13	0.448
2-methylbut-1-ene	alkene	92	10	6.26	5	61.00	70.13	0.870
3-methylbut-1-ene	alkene	89	17	6.79	5	31.40	70.13	0.448
2-methylbut-2-ene	alkene	155	35	13.81	5	86.00	70.13	1.226
butylene	alkene	97	12	6.18	4	50.80	56.11	0.905
isoprene	alkene	173	19	10.33	5	99.60	68.12	1.462
hex-1-ene	alkene	92	13	5.31	6	37.00	84.16	0.440
cis-hex-2-ene	alkene	127	30	8.10	6	66.00	84.16	0.784
trans-hex-2-ene	alkene	127	30	8.41	6	66.00	84.16	0.784
1,3-butadiene	alkene	120	12	12.28	4	65.90	54.09	1.218
alpha-pinene	alkene	109	20	4.40	10	51.80	136.23	0.380
beta-pinene	alkene	70	16	3.40	10	73.50	136.23	0.540
acrolein	alkene	80	44	7.27	3	19.90	56.06	0.355
methacrolein	alkene	136	41	5.86	4	28.40	70.09	0.405
limonene	alkene	134	31	4.43	10	163.00	136.23	1.197
formaldehyde	aldehyde	78	20	9.28	1	8.47	30.03	0.2821
acetaldehyde	aldehyde	59	20	6.37	2	14.90	44.05	0.3383
propionaldehyde	aldehyde	63	24	6.86	3	19.70	58.08	0.3392
butyraldehyde	aldehyde	60	21	5.78	4	23.50	72.11	0.3259
i-butyraldehyde	aldehyde	60	18	5.08	4	26.80	72.11	0.3717
pentanal	aldehyde	74	20	4.91	5	27.80	86.13	0.3228
3-methylbutanal	aldehyde	73	23	4.81	5	27.00	86.13	0.3135
glyoxal	aldehyde	60	16	12.20	2	11.00	58.04	0.1895
methylglyoxal	aldehyde	163	44	16.11	3	15.00	72.06	0.2082

acetone	ketone	4	1	0.35	3	0.19	58.08	0.0033
methylethylketone	ketone	18	4	1.44	4	1.20	72.11	0.0166
diethylketone	ketone	17	5	1.18	5	2.00	86.13	0.0232
methyl-i-butylketone	ketone	53	6	3.76	6	12.70	100.16	0.1268
benzene	aromatic	1	6	0.70	6	1.22	78.11	0.0156
toluene	aromatic	33	8	3.90	7	5.58	92.14	0.0606
o-xylene	aromatic	79	19	7.48	8	13.60	106.17	0.1281
m-xylene	aromatic	94	23	9.57	8	23.10	106.17	0.2176
p-xylene	aromatic	74	17	5.72	8	14.30	106.17	0.1347
ethylbenzene	aromatic	36	9	2.95	8	7.00	106.17	0.0659
propylbenzene	aromatic	26	6	1.96	9	5.80	120.19	0.0483
i-propylbenzene	aromatic	29	6	2.44	9	6.30	120.19	0.0524
1,2,3-trimethylbenzene	aromatic	125	32	11.73	9	32.70	120.19	0.2721
1,2,4-trimethylbenzene	aromatic	137	27	8.69	9	32.50	120.19	0.2704
1,3,5-trimethylbenzene	aromatic	141	23	11.50	9	56.70	120.19	0.4718
o-ethyltoluene	aromatic	65	18	5.46	9	11.90	120.19	0.0990
m-ethyltoluene	aromatic	82	19	7.25	9	18.60	120.19	0.1548
p-ethyltoluene	aromatic	60	16	4.34	9	11.80	120.19	0.0982
3,5-dimethylethylbenzene	aromatic	134	24	9.85	10	57.70	134.22	0.4299
1,2,3,5-tetramethylbenzene	aromatic	188	49	9.06	10		134.22	
1,2,4,5-tetramethylbenzene	aromatic	181	47	9.06	10		134.22	
1-methyl-3-i-propylbenzene	aromatic	151	44	6.96	10	25.50	134.22	0.1900
3,5-diethyltoluene	aromatic	121	25	8.70	11	59.30	148.24	0.4000
benzaldehyde	aromatic	-36	34	-0.68	6	12.00	106.12	0.1131
2-methylbenzaldehyde	aromatic	-101	83	-0.60	7		120.15	
3-methylbenzaldehyde	aromatic	-83	69	-0.60	7		120.15	
4-methylbenzaldehyde	aromatic	-36	43	-0.60	7		120.15	
styrene	aromatic	7	31	1.65	8	58.00	104.15	0.5569
phenol	aromatic	-119	166	2.70	6		94.11	

o-cresol	aromatic	-20	116	2.35	7	40.30	108.14	0.3727
2,5-xyleneol	aromatic	42	115	2.08	8		122.16	
2,4-xyleneol	aromatic	52	95	2.08	8		122.16	
2,3-xyleneol	aromatic	16	105	2.08	8		122.16	
methanol	alcohol	8	1	0.66	1	0.90	32.04	0.0282
ethanol	alcohol	17	5	1.46	2	3.21	46.07	0.0697
i-propanol	alcohol	13	2	0.59	3	5.09	60.10	0.0847
propanol	alcohol	30	6	2.40	3	5.81	60.10	0.0967
butanol	alcohol	35	8	2.77	4	8.45	74.12	0.1140
i-butanol	alcohol	34	2	2.42	4	9.30	74.12	0.1255
sec-butanol	alcohol	26	5	1.30	4	8.70	74.12	0.1174
3-methyl-1-butanol	alcohol	47	3	3.06	5	13.00	88.15	0.1475
diacetone alcohol	alcohol	21	3	0.57	6	1.49	116.16	0.0128
methyl formate	ester	1	0	0.05	2	0.23	60.05	0.0038
methyl acetate	ester	3	1	0.07	3	0.35	74.08	0.0047
ethyl acetate	ester	11	2	0.60	4	1.60	88.11	0.0182
i-propyl acetate	ester	16	3	1.03	5	3.40	102.13	0.0333
n-propyl acetate	ester	15	3	0.74	5	3.40	102.13	0.0333
butyl acetate	ester	14	2	0.79	6	4.20	116.16	0.0362
dimethylether	ether	18	5	0.76	2	2.83	46.07	0.0614
diethylether	ether	53	9	3.63	4	13.10	74.12	0.1767
di-i-propylether	ether	41	8	3.41	6	32.80	102.17	0.3210
formic acid	acid	1	0	0.06	1	0.45	46.03	0.0098
acetic acid	acid	6	1	0.67	2	0.73	60.05	0.0121
propanoic acid	acid	6	2	1.18	3		74.08	
ethylene glycol	oxygenate	25	5	3.03	2	14.70	62.07	0.2368
propylene glycol	oxygenate	29	7	2.49	3	21.50	76.09	0.2826
2-butoxyethanol	oxygenate	38	7	2.79	6	25.70	118.17	0.2175
1-methoxy-2-propanol	oxygenate	32	6	2.34	4	20.00	90.12	0.2219

2-methoxyethanol	oxygenate	34	3	2.84	3	13.30	76.09	0.1748
2-ethoxyethanol	oxygenate	42	5	3.59	4	18.70	90.12	0.2075
acetylene	alkyne	4	0	0.94	2	0.77	26.04	0.0296
propyne	alkyne	101	40	6.61	3	5.90	40.06	0.1473
cyclohexane	cycloalkane	20	5	1.16	6	7.02	84.16	0.0834
cyclohexanone	cycloalkane	21	5	1.27	6	6.40	98.14	0.0652
cyclohexanol	cycloalkane	45	10	1.84	6	19.00	100.16	0.1897
methylene dichloride	halocarbon	1	1	0.04	2	0.15	84.93	0.0017
tetrachloroethylene	halocarbon	1	0	0.03	2	0.17	165.83	0.0010
trichloroethylene	halocarbon	14	3	0.61	2	2.34	131.39	0.0178
ethyl chloride	halocarbon	12	5	0.27	2	0.42	64.51	0.0065
ethylidene dichloride	halocarbon	91	22	1.69	2	10.90	96.94	0.1124

Notes

- ethylene is the index point of the POCP scale which is by definition 100 with a standard deviation of zero. This does not imply that the reactivity of ethylene is completely certain, merely that all other POCPs have been expressed relative to ethylene = 100.
- Data taken from Calvert et al., 2000; 2002; 2008) and Carter, 2008.
- rate coefficients multiplied by 10^{12} in unit of $\text{cm}^3 \text{ molecule}^{-1} \text{ s}^{-1}$.